Macromolecules

ARTICLE

pubs.acs.org/Macromolecules

Narrow or Monodisperse, Highly Cross-Linked, and "Living" Polymer Microspheres by Atom Transfer Radical Precipitation Polymerization

Jingshuai Jiang, Ying Zhang, Xianzhi Guo, and Huiqi Zhang*

Key Laboratory of Functional Polymer Materials (Nankai University), Ministry of Education, and Department of Chemistry, Nankai University, Tianjin 300071, People's Republic of China

Supporting Information

ABSTRACT: A facile, general, and efficient one-pot approach to obtaining narrow or monodisperse, highly cross-linked, surface-functionalized, and "living" polymer microspheres with uniformly cross-linked structures by atom transfer radical precipitation polymerization (ATRPP) is described for the first time. The simple introduction of atom transfer radical polymerization (ATRP) mechanism into precipitation polymerization system allows the direct generation of uniformly cross-linked "living" polymer microspheres with their number-average diameters ranging from 0.73 to 3.25 μm and their polydispersity indices being typically lower than 1.01. The polymerization parameters (including stirring rate, monomer loading, initiator and catalyst concentrations, molar ratio of cross-linker to monovinyl functional comonomer, and polymerization scale and time) have proven to show significant influence on the morphologies of the resulting polymer microspheres, which makes it very convenient to control the particle sizes by easily tuning the reaction conditions. The general applicability of ATRPP was demonstrated by synthesizing a series of uniform functional copolymer microspheres with different incorporated functional comonomers (i.e, 4-vinylpyridine, acrylamide, and 2-hydroxyethyl methacrylate). Moreover, the "livingness" of the resulting polymer microspheres was confirmed by their direct grafting of hydrophilic polymer brushes via surface-initiated ATRP under mild reaction conditions. Furthermore, a "grafting from" particle growth mechanism is proposed for ATRPP, which is considerably different from the "grafting to" particle growth mechanism in the traditional precipitation polymerization.

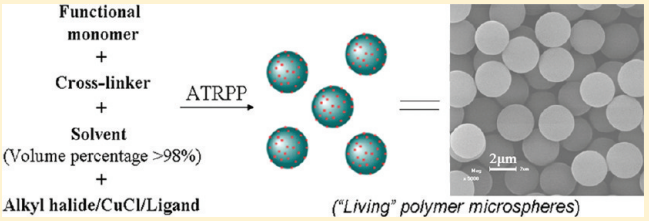

INTRODUCTION

Recent years have witnessed considerable interest in narrow or monodisperse highly cross-linked spherical polymer particles in the micrometer-size range due to their great potential in a wide range of materials science applications.[1−5] Among various approaches presently available for obtaining such polymer microspheres, precipitation polymerization has received particular attention because of its easy operation and no need for any surfactant or stabilizer.[6−24] So far, several different kinds of precipitation polymerization approaches based on the conventional free radical mechanism have been developed for the preparation of uniform highly cross-linked spherical polymer particles, such as traditional precipitation polymerization,[7−12,14−17,21,22,24] distillation precipitation polymerization,[13,18] and photoinduced precipitation polymerization.[19,20,23] One of the main present focuses in this rapidly growing field is the development of facile and versatile approaches for the efficient preparation of advanced functional polymer microspheres.[5]

Two main strategies have been developed for the above purpose up to now, where the first one involves the direct preparation of functional polymer microspheres by copolymerizing monovinyl functional monomers with cross-linkers via precipitation polymerization,[8,12,16,18,23] and the second one is realized by grafting functional polymer layers onto the polymer particles prepared by precipitation polymerization.[25−34] While the first strategy usually requires rather time-consuming optimization of polymerization parameters for obtaining uniform functional polymer microspheres, the second one allows the facile grafting of all the functional monomers onto the surfaces of the preformed polymer particles, thus leading to their flexible preparation and more efficient functionalization. In particular, the functional polymer brushes grafting strategy has proven to be one of the most efficient approach for the functionalization of polymer microspheres, which includes "grafting to" and "grafting from" approaches.[5] While the former one is based on the covalent attachment of the preformed functional polymer chains with an active terminal group to a surface bearing corresponding reactive functional groups, the later one allows growing functional polymer chains from the initiating groups on the substrate surfaces by the surface-initiated polymerization of functional monomers. In comparison with the "grafting to" approach, the "grafting from" approach has the advantage of obtaining high grafting densities because the functional monomers can easily diffuse to the propagating sites of the substrate surfaces.[5] Many controlled "grafting from" techniques have been developed up to now, where controlled/"living" radical polymerization techniques

Received: May 6, 2011
Revised: June 28, 2011
Published: July 15, 2011

(CRPs) (e.g., nitroxide-mediated radical polymerization,[35] atom transfer radical polymerization (ATRP),[36,37] and reversible addition−fragmentation chain transfer (RAFT) polymerization[38]) have been most widely utilized due to their good control over the polymer architectures, broad applicability to a wide range of monomers, and rather mild reaction conditions. In all cases, the presence of CRP-"living" groups on the surfaces of polymer particles is necessary. The spherical polymer particles prepared by traditional precipitation polymerization, however, normally do not have such "living" groups, which makes their further surface modification necessary to introduce the required "living" groups prior to their surface functionalization.[25−28] Evidently, the development of facile and versatile approaches for the one-pot preparation of narrow or monodisperse, highly cross-linked, and "living" polymer beads would permit the more efficient synthesis of advanced functional polymer materials with improved quality and expanded applications, and it is thus of great importance.

It is well-known that CRPs can provide well-defined polymers with end-capped "living" groups.[35−38] Therefore, it can be anticipated that the introduction of CRP mechanism into the traditional polymer beads-forming approaches should allow the synthesis of spherical polymer particles with "living" groups on their surfaces (i.e., "living" polymer beads). While some un-cross-linked or lightly cross-linked "living" spherical polymer particles have been prepared on the basis of the above principle by applying various CRPs in dispersed polymerization systems[39−48] (including the preparation of monodisperse un-cross-linked or lightly cross-linked polymer microspheres by two-stage living radical dispersion polymerizations[40,44]), *the preparation of narrow or monodisperse, highly cross-linked, and "living" polymer microspheres still remains a significant challenge.*[44] It is only recently that several attempts have been tried for exploring the possibility of synthesis of highly cross-linked "living" spherical polymer particles by the combined use of CRPs and precipitation polymerization technique.[29,33,34,49] Barner and co-workers described the preparation of highly cross-linked "living" polymer microspheres with surface-immobilized RAFT groups by RAFT agent-mediated precipitation polymerization (or RAFT precipitation polymerization) and narrow-disperse polymer particles were claimed to be obtained.[29] However, the quite large coefficient of variation (CV) value reported for the obtained particles (CV = 29.5) suggested that they were still quite polydisperse.[23] In addition, our recent results also showed that RAFT precipitation polymerization only resulted in highly cross-linked "living" polymer microspheres with broad size distributions.[34,49] Recently, our group has succeeded in preparing uniform highly cross-linked "living" polymer microspheres by using iniferter-induced "living" radical precipitation polymerization through the adaption of iniferter-induced "living" radical polymerization mechanism[50] into precipitation polymerization system.[33] However, the controllability of iniferter-induced "living" radical polymerization is known to be inferior to other CRPs (e.g., ATRP and RAFT polymerization), which may not meet the requirement for the well-controlled surface functionalization processes. In addition, only polydisperse functional copolymer microspheres were obtained by using the above technique.

In this paper, we demonstrate that narrow or monodisperse, highly cross-linked, surface-functionalized, and "living" polymer microspheres with uniformly cross-linked structures can be successfully prepared via atom transfer radical precipitation polymerization (ATRPP) by introducing ATRP mechanism into precipitation polymerization in a facile and highly efficient one-pot approach. *To the best of our knowledge, the findings we describe here represent the first successful preparation of such advanced functional "living" polymer microspheres with a great potential for various materials science applications.* The effects of the polymerization parameters on the morphologies and yields of the polymer particles were studied. In addition, the general applicability of ATRPP, the "livingness" of the obtained polymer microspheres, and the particle growth mechanism in ATRPP were also investigated.

EXPERIMENTAL SECTION

Materials. 4-Vinylpyridine (4-VP, Alfa Aesar, 96%) and ethylene glycol dimethacrylate (EGDMA, Alfa Aesar, 98%) were purified by distillation under vacuum. Acetonitrile (Tianjin Jiangtian Chemicals, China, analytical grade (AR)) was distilled over CaH_2 prior to use. Tetrahydrofuran (THF, Tianjin Jiangtian Chemicals, 99%) was refluxed over sodium and then distilled. Copper(I) chloride (CuCl, Tianjin Jiangtian Chemicals, AR) was purified by stirring it with acetic acid for 12 h, washed with ethanol and diethyl ether, and then dried under vacuum at 75 °C for 3 days. Tris[2-(dimethylamino)ethyl]amine (Me_6TREN) was prepared by a one-step synthesis procedure from commercially available tris(2-aminoethyl)amine (Acros, 97%) according to a reported procedure.[51] 2-Hydroxyethyl methacrylate (HEMA, Tianjin Institute of Chemical Reagents, China, chemical pure) was purified by washing its aqueous solution (25 vol % of HEMA) with hexanes (4 × 200 mL), salting it out of the aqueous phase by addition of NaCl, drying over $MgSO_4$, and distilling under reduced pressure. Acrylamide (AAm, Tianjin Jiangtian Chemicals, 98+%) was recrystallized from acetone before use. *N*-Isopropylacrylamide (NIPAAm, Acros, 99%) was purified by recrystallization from hexane. *N*,*N*,*N*′,*N*″,*N*″-Pentamethyldiethylenetriamine (PMDETA, Aldrich, 99%), anhydrous copper(II) chloride ($CuCl_2$, Alfa Aesar, 98%), copper(II) bromide ($CuBr_2$, Alfa Aesar, 99%), 2,2′-bipyridine (Tianjin Jiangtian Chemicals, 99.5+%), ethyl 2-chloropropionate (Alfa Aesar, 97%), Rhodamine B (Alfa Aesar, 98%), *N*,*N*′-dicyclohexylcarbodiimide (DCC, Tianjin Jiangtian Chemicals, AR), 4-(dimethylamino)pyridine (DMAP, Merck, AR), and all the other chemicals were used as received unless otherwise stated.

Preparation of Highly Cross-Linked Poly(4-VP-*co*-EGDMA) Microspheres by ATRPP. The recipes for the ATRPP of 4-VP with EGDMA in acetonitrile are listed in Table 1. A typical procedure is presented as follows: To a one-neck round-bottom flask (50 mL) with a magnetic stir bar inside, CuCl (1.30 mg, 0.0131 mmol), 4-VP (30.70 mg, 0.2920 mmol), EGDMA (231.30 mg, 1.1679 mmol), and dried acetonitrile (30 mL) were added successively. The reaction mixture was purged with argon for 15 min and then PMDETA (4.55 mg, 0.02625 mmol) was added. After another 15 min of argon bubbling, ethyl 2-chloropropionate (1.80 mg, 0.01313 mmol) was added into the system. The flask was then sealed, immersed into a thermostated oil bath at 60 °C, and stirred for 24 h with a magnetic stir bar at a stirring rate of 130 rpm. The resulting polymer particles were separated by centrifugation and washed with methanol five times to remove the copper catalyst, which were then dried at 40 °C under vacuum overnight to provide a white powder (yield: 46%).

A series of other highly cross-linked polymer microspheres were also prepared similarly following the above procedure by changing the reaction parameters including the stirring rate, monomer loading, initiator and catalyst concentrations, molar ratio of the cross-linker to comonomer, and polymerization scale and time (Table 1).

Preparation of Poly(HEMA-*co*-EGDMA) Microspheres by ATRPP. To a one-neck round-bottom flask (50 mL) with a magnetic stir bar inside were added CuCl (0.98 mg, 0.00984 mmol), HEMA (51.29 mg, 0.3941 mmol), EGDMA (155.50 mg, 0.7856 mmol), and dried

Table 1. Synthetic and Characterization Data for the Polymer Microspheres Prepared by the ATRPP of a monovinyl functional monomer (4-VP, HEMA, or AAm) and EGDMA under Different Reaction Conditions[a]

entry	stirring rate (rpm)	polym time (h)	EGDMA/FM/initiator/CuCl/PMDETA (molar ratio)[b]	FM[b] + EGDMA (vol %)	solvent (mL)	yield (%)	D_n[d] (μm)	U[d]	CV[e] (%)
1	**0**	24	100/25/1.125/1.125/2.25	0.8	30	43	2.40	1.238	26.5
2	**90**	24	100/25/1.125/1.125/2.25	0.8	30	44	2.25	1.004	4.3
3	**130**	24	100/25/1.125/1.125/2.25	0.8	30	45	2.82	1.004	4.1
4	**130**	24	100/25/1.125/1.125/2.25	0.8	30	44	2.82	1.004	4.2
5	**130**	24	100/25/1.125/1.125/2.25	0.8	30	46	2.83	1.004	4.3
6	**180**	24	100/25/1.125/1.125/2.25	0.8	30	48	2.84	1.007	5.4
7	**230**	24	100/25/1.125/1.125/2.25	0.8	30	49	2.90	1.007	5.1
8	130	24	100/25/1.125/1.125/2.25	**0.6**	30	34	1.52	1.009	5.7
9	130	24	100/25/1.125/1.125/2.25	**0.8**	30	45	2.82	1.004	4.1
10	130	24	100/25/1.125/1.125/2.25	**1.0**	30	48	3.19	1.009	5.5
11	130	24	100/25/1.125/1.125/2.25	**1.2**	30	50	2.66	1.205	24.1
12	130	13	100/25/1.125/1.125/2.25	**1.2**	30	34	2.64	1.003	3.5
13	130	7	100/25/1.125/1.125/2.25	**1.4**	30	26	1.86	1.007	4.8
14	130	24	100/25/**1.500**/1.125/2.25	0.8	30	49	3.01	1.004	3.8
15	130	24	100/25/**1.406**/1.125/2.25	0.8	30	47	2.88	1.003	3.6
16	130	24	100/25/**1.125**/1.125/2.25	0.8	30	45	2.82	1.004	4.1
17	130	24	100/25/**0.844**/1.125/2.25	0.8	30	43	2.81	1.018	6.8
18	130	24	100/25/1.125/**1.500**/**3.00**	0.8	30	51	3.25	1.007	4.8
19	130	24	100/25/1.125/**1.406**/**2.81**	0.8	30	49	2.85	1.011	5.7
20	130	24	100/25/1.125/**1.125**/**2.25**	0.8	30	45	2.82	1.004	4.1
21	130	24	100/25/1.125/**0.843**/**1.69**	0.8	30	33	2.15	1.006	4.6
22	130	24	**100**/**25**/1.125/1.125/2.25	0.8	30	45	2.82	1.004	4.1
23	130	24	**100**/**33**/1.165/1.165/2.33	0.8	30	38	2.88	1.003	3.3
24	130	24	**100**/**50**/1.250/1.250/2.50	0.8	30	35	2.96	1.012	7.0
25	130	24	**100**/**100**/1.50/1.50/3.00	0.8	30	25	1.90	1.285	31.0
26	130	24	100/25/1.125/1.125/2.25	0.8	**30**	45	2.82	1.004	4.1
27	130	24	100/25/1.125/1.125/2.25	0.8	**60**	38	2.50	1.004	3.8
28	130	24	100/25/1.125/1.125/2.25	0.8	**120**	35	2.38	1.008	5.3
29	130	**2**	100/25/1.125/1.125/2.25	0.8	30	3	0.73	1.022	8.6
30	130	**3**	100/25/1.125/1.125/2.25	0.8	30	5	1.02	1.015	6.9
31	130	**6**	100/25/1.125/1.125/2.25	0.8	30	12	1.55	1.006	4.7
32	130	**12**	100/25/1.125/1.125/2.25	0.8	30	23	2.15	1.006	4.7
33	130	**18**	100/25/1.125/1.125/2.25	0.8	30	35	2.53	1.006	4.3
34	130	**24**	100/25/1.125/1.125/2.25	0.8	30	46	2.83	1.004	4.3
35	130	24	100/50/1.250/1.250/2.50	0.65	30	31	1.25	1.024	8.9
36	130	24	100/25/1.125/1.125/2.25	0.6[c]	30	33	2.60	1.005	4.1

[a] All the polymerizations were performed at 60 °C in acetonitrile. [b] FM refers to the monovinyl functional monomer, which is 4-VP for entries 1−34, HEMA for entry 35, and AAM for entry 36, respectively, and initiator is ethyl 2-chloropropionate. [c] The volume of AAm was calculated by dividing its weight to its density. [d] D_n and U are the number-average diameter and polydispersity index of the polymer microspheres, respectively. [e] CV denotes the coefficient of variation of the polymer particles.

acetonitrile (30 mL) successively. The reaction mixture was purged with argon for 15 min, and then PMDETA (3.41 mg, 0.01969 mmol) was added. After another 15 min of argon bubbling, ethyl 2-chloropropionate (1.344 mg, 0.00984 mmol) was added into the system. The flask was then sealed, immersed into a thermostated oil bath at 60 °C, and stirred for 24 h with a magnetic stir bar at a stirring rate of 130 rpm. The resulting polymer particles were separated by centrifugation and washed with methanol several times to remove the copper catalyst, which were then dried at 40 °C under vacuum overnight (yield: 31%).

Preparation of Poly(AAm-*co*-EGDMA) Microspheres by ATRPP. To a one-neck round-bottom flask (50 mL) with a magnetic stir bar inside, CuCl (0.98 mg, 0.00984 mmol), AAm (15.56 mg, 0.2190 mmol), EGDMA (173.40 mg, 0.8759 mmol), and dried acetonitrile (30 mL) were added successively. The reaction mixture was purged with argon for 15 min and then PMDETA (3.41 mg, 0.01969 mmol) was added. After another 15 min of argon bubbling, ethyl 2-chloropropionate (1.34 mg, 0.00984 mmol) was added into the system. The flask was then sealed, immersed into a thermostated oil bath at 60 °C, and stirred for 24 h with a magnetic stir bar at a stirring rate of 130 rpm. The resulting polymer particles were separated by centrifugation and washed with methanol several times to remove the copper catalyst, which were then dried at 40 °C under vacuum overnight (yield: 33%).

Grafting Polymer Brushes onto Polymer Microspheres. Poly(NIPAAm) (i.e., PNIPAAm) brushes were grafted onto the above-obtained polymer microspheres according to the following procedure: Polymer microspheres with surface-bound ATRP initiating groups

(i.e., the sample entry 28 in Table 1) (50 mg), NIPAAm (0.34 g, 3 mmol), CuCl (5.00 mg, 0.05 mmol), $CuCl_2$ (0.68 mg, 0.005 mmol), and isopropanol (2 mL) were added into a one-neck round-bottom flask (25 mL) successively. After the reaction mixture was degassed by bubbling argon for 15 min in an ice-bath, Me_6TREN (12.40 mg, 0.054 mmol) was added. After another 15 min of argon bubbling, the reaction mixture was sealed. The polymerization was performed at ambient temperature with stirring for 24 h. After centrifugation, the resulting solid product was thoroughly washed with methanol to remove the copper catalyst and then dried at 25 °C under vacuum to a constant weight, leading to the grafted polymer microspheres with a weight of 55 mg.

Poly(HEMA) (i.e., PHEMA) brushes were grafted onto the polymer microspheres according to the following procedure: Polymer microspheres with surface-bound ATRP initiating groups (the sample entry 28 in Table 1) (50 mg), HEMA (0.95 g, 7.3 mmol), CuCl (7.23 mg, 0.073 mmol), $CuBr_2$ (4.89 mg, 0.0219 mmol), methanol (1 mL), and distilled water (1 mL) were added into a one-neck round-bottom flask (25 mL) successively. After the reaction mixture was degassed by bubbling argon for 15 min in an ice-bath, 2,2′-bipyridine (31.93 mg, 0.2044 mmol) was added. After another 15 min of argon bubbling, the reaction mixture was sealed. The polymerization was carried out at ambient temperature with stirring for 24 h. After centrifugation, the resulting solid product was thoroughly washed with methanol to remove the copper catalyst and then dried at 25 °C under vacuum to a constant weight, leading to grafted polymer microspheres with a weight of 56 mg.

Fluorescent Labeling of Polymer Microspheres with Grafted PHEMA Brushes. The fluorescent labeling of polymer microspheres with grafted PHEMA brushes was achieved by the esterification reaction between the hydroxyl groups of PHEMA brushes and the carboxyl group of the fluorescent dye Rhodamine B following a typical procedure as shown below: Polymer microspheres with grafted PHEMA brushes (4 mg) were added into a solution of Rhodamine B (20 mg, 0.042 mmol), DCC (8.57 mg, 0.042 mmol), and DMAP (1.71 mg, 0.014 mmol) in dried THF (4 mL), and the reaction mixture was stirred at 25 °C for 8 h. After centrifugation, the resulting solid product was thoroughly washed with methanol/acetic acid (9/1 v/v), THF/acetic acid (9/1 v/v), and then methanol successively to remove the excessive Rhodamine B until no fluorescence was detectable for the centrifugated supernatant, which was then dried at room temperature under vacuum overnight, leading to a purple product with a yield of 98%.

As a control experiment, the ungrafted polymer microspheres were submitted to the same labeling conditions.

Characterizations. Fourier transform infrared (FT-IR) spectra of the polymer microspheres were measured with a Bio-Rad FTS-6000 spectrometer.

The morphologies, particle sizes, and size distributions of the polymer microspheres were determined with a scanning electron microscope (SEM, Shimadzu SS-550). All of the SEM size data reflect the averages of more than 100 particles, which are calculated by the following formulas:[7,13]

$$D_n = \sum_{i=1}^{k} n_i D_i / \sum_{i=1}^{k} n_i; D_w = \sum_{i=1}^{k} n_i {D_i}^4 / \sum_{i=1}^{k} n_i {D_i}^3;$$

$$U = D_w/D_n; \quad CV = [\sum_{i=1}^{k} (D_i - D_n)^2/(k-1)]^{1/2}/D_n$$

where D_n is the number-average diameter, D_w the weight-average diameter, U the size distribution index, CV the coefficient of variation, k the total number of the measured particles, D_i the particle diameter of the ith polymer microsphere, and n_i the particle number of the microspheres with a diameter D_i.

The confocal fluorescence microscopy images of the polymer microspheres were obtained with a Leica TCS SP5 confocal laser scanning microscope. All images were taken by using an oil immersion lens NA 1.4 (Objective HCX PL APO CS 63.0 × 1.4 oil) with a 543 nm He−Ne laser as the excitation light.

The dispersion properties of the polymer microspheres in pure water were studied as follows: The suspensions of the polymer microspheres in pure water (1 mg/mL) were first dispersed by ultrasonic, and they were then allowed to settle down for a certain time at 20 °C to check their dispersion stability.

The static contact angle measurements for the polymer films were performed according to the following procedure: The films of the polymer microspheres were prepared by casting their suspension solutions in *N*,*N*-dimethylformamide (10 mg/mL, after ultrasonic dispersion) on clean glass surfaces. After the solvent was allowed to evaporate at ambient temperature overnight, the formed polymer films were further dried under vacuum for 24 h. A KRÜSS FM40 Easy Drop contact angle equipment (Germany) was utilized to determine their static water contact angles. Two measurements were taken across each sample, with their average being used for analysis.

RESULTS AND DISCUSSION

Surface-initiated ATRP has proven to be highly robust in the controlled functionalization of various substrates by the facile surface-grafting of functional polymer brushes[52] or cross-linked layers.[53] It can thus be envisioned that the development of facile and versatile approaches for the direct preparation of narrow or monodisperse, highly cross-linked, and "living" polymer microspheres with ATRP initiating groups on their surfaces would pave the way for their broad applications in the field of materials science. In a recent paper, we described our first attempt in the preparation of such polymer microspheres by the combined use of ATRP and precipitation polymerization technique (i.e., ATRPP) without stirring the polymerization system both in the presence and in the absence of a template molecule (e.g., bisphenol A), but the resulting polymer microspheres were rather polydisperse.[54] More recently, we succeeded in preparing uniform highly cross-linked poly(EGDMA) microspheres by using iniferter-induced "living" radical precipitation polymerization, where the application of magnetic stirring during the polymerization process proved to play a decisive role in generating uniform polymer microspheres.[33] Inspired by this encouraging result, we returned back to the ATRPP system and tried to check whether it can be used to prepare uniform, highly cross-linked, and "living" polymer microspheres by optimizing the polymerization parameters by this technique (e.g., by stirring the polymerization solutions). In addition, the general applicability of ATRPP, the "livingness" of the resulting polymer microspheres, and the particle formation mechanism in ATRPP were also investigated.

Effects of Polymerization Parameters on the Morphologies and Yields of the Resulting Polymer Microspheres. ATRPP involves the introduction of ATRP mechanism into precipitation polymerization system, which can be implemented by simply replacing the initiator normally used in the traditional precipitation polymerization (e.g., AIBN) with an ATRP initiating system (e.g., an alkyl halide and a transition-metal complex formed by a transition metal in its lower oxidation state and a ligand[55]). A model system was chosen here to demonstrate the proof-of-principle, which utilized 4-VP, EGDMA, ethyl 2-chloropropionate, CuCl, PMDETA, and acetonitrile as the monovinyl functional monomer, divinyl cross-linking monomer, initiator, transition metal salt, ligand, and solvent, respectively. The incorporation of functional monomers into the polymerization system can lead to copolymer microspheres with extra surface-immobilized functional groups, which should make them more

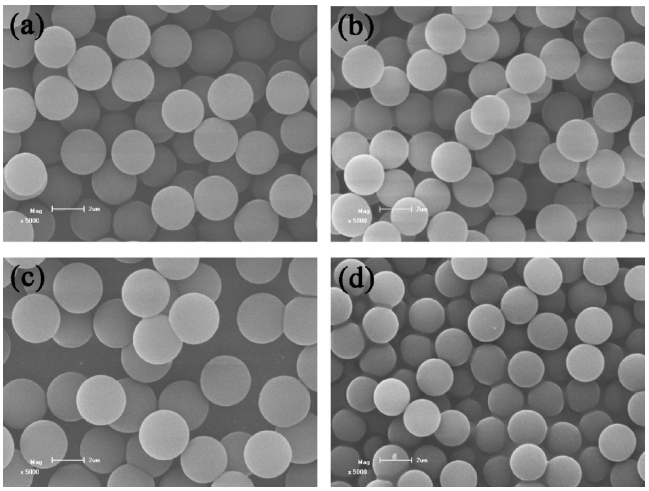

Figure 1. SEM images of the representative poly(4-VP-*co*-EGDMA) microspheres prepared by ATRPP at a stirring rate of 130 rpm (the samples a, b, c, and d correspond to entries 3, 12, 18, and 28 in Table 1, respectively). The scale bar corresponds to 2 μm in parts a−d.

useful for many applications. For example, gold-immobilized polymer microspheres have been prepared by using the polymer particles with pyridine groups.[42]

The control over the size and uniformity of the polymer particles is of extreme importance for their potential applications and has been the major area of interest.[24] Therefore, the studies on their influencing parameters are of significant importance, in particular for a new precipitation polymerization system. In the following parts, the effects of various polymerization parameters on the morphologies and yields of the polymer particles prepared via ATRPP were studied, including stirring rate, monomer loading, initiator and catalyst concentrations, molar ratio of the cross-linker to monovinyl functional monomer, and polymerization scale.

(1). Effect of Stirring Rate. It has been demonstrated previously that narrow or monodisperse highly cross-linked polymer microspheres can be readily prepared by traditional precipitation polymerization either under gentle agitation[7−12,14−17,19−23] or without any stirring.[24,56] However, some recent studies showed that the presence of stirring was critical for the preparation of uniform polymer microspheres in some precipitation polymerization systems.[14,33] Therefore, a series of ATRPP experiments were first carried out at different magnetic stirring rates (i.e., 0, 90, 130, 180, and 230 rpm) to check whether narrow or monodisperse polymer microspheres can be prepared via ATRPP under the optimal stirring rates (Table 1, entries 1−7). The results showed that while the polymer particles prepared in the absence of magnetic stirring (i.e., the stirring rate was 0 rpm) were rather polydisperse (Figure S1a in the Supporting Information, entry 1 in Table 1), monodisperse polymer microspheres with smooth surfaces were obtained by applying appropriate stirring rates (90−180 rpm) under the otherwise same conditions (Figure 1a, Figure S1b−d in the Supporting Information). It was observed that most of the polymer particles were precipitated onto the bottom of the round-bottom flask at the end of ATRPP in the absence of any stirring, whereas homogeneous milky solutions were achieved under the magnetic stirring, revealing that appropriate stirring significantly improved the suspension stability of the polymer particles in the reaction medium, which should be responsible for the formation of monodisperse polymer microspheres. A further increase in the stirring rate up to 230 rpm, however, resulted in polymer microspheres with some of them having uneven shapes (Figure S1e in the Supporting Information), suggesting the occurrence of some coagulation of polymer particles during their nucleation or growth processes due to the too fast stirring rate. The number-average diameters (i.e., D_n) of the polymer microspheres increased from 2.25 to 2.82 μm with increasing the stirring rate from 90 to 130 rpm, which could be attributed to the increased possibility of coagulation among the primary particle nuclei in the initial stage of the polymerization with an increase in the stirring rate, leading to the reduced number of final polymer nuclei and thus larger particles. A further increase in the stirring rate from 130 to 180 rpm proved to lead to monodisperse polymer microspheres with almost the same particle sizes. This, together with their comparable yields, suggested that the polymer particle formation processes were not sensitive to the agitation any more when the stirring rates were in a high enough and appropriate range. On the basis of the above results, a stirring rate of 130 rpm was chosen for all the following ATRPP studies unless otherwise stated. It is worth mentioning here that three repetition ATRPP experiments were performed with a stirring rate of 130 rpm and totally reproducible data were obtained (entries 3−5 in Table 1, Figure S2 in the Supporting Information), thus demonstrating the reliability of the experimental results.

(2). Effect of Monomer Loading. To understand more about ATRPP, the effect of monomer loading on the morphologies and yields of the polymer particles was also studied, where a series of ATRPP experiments with different monomer concentrations in the reaction media were performed with the other polymerization parameters (including the stirring rate, reactant composition, polymerization temperature, and polymerization time (24 h)) being held constant (Table 1, entries 8−11). The SEM characterization showed that narrow or monodisperse poly(4-VP-*co*-EGDMA) microspheres with smooth surfaces were formed when the amount of the monomers used (including both EGDMA and 4-VP) was varied from 0.6 to 1.0 vol % (relative to the total reaction medium) (Figure S3a−c in the Supporting Information). Both the sizes and yields of the polymer microspheres increased with increasing the monomer loadings, just as observed in the traditional precipitation polymerization system.[13] For example, the D_n values of the polymer microspheres increased from 1.52 μm for a monomer loading of 0.6 vol % (Table 1, entry 8) to 3.19 μm for a monomer loading of 1.0 vol % (Table 1, entry 10), and the yields of the corresponding polymer microspheres increased from 34 to 48% in the meantime. The increase in the sizes of the polymer microspheres might be attributed to the increase in the solubility of the initially formed branched oligomers with increasing monomer loadings, which allows the oligomers with relatively higher molecular weights still soluble in the reaction media, leading to a decrease in the amount of particle nuclei and thus larger particle sizes.[14,21] When the monomer loading was increased to 1.2 vol %, polymer particles started to precipitate onto the bottom of the reaction flask after 13.5 h, leading to polydisperse polymer microspheres (Figure S3d in the Supporting Information). Shortening the polymerization time to 13 h in the above reaction, however, resulted in monodisperse polymer microspheres (Figure 1b, entry 12 in Table 1). A further increase in monomer loading up to 1.4 vol % provided monodisperse polymer microspheres at a polymerization time of 7 h (Figure S3f in the Supporting

Information, entry 13 in Table 1). It is worth pointing out here that in comparison with the monomer loadings normally utilized in the traditional precipitation polymerization (where narrow-disperse polymer microspheres can be prepared by using up to 5 vol % monomer loadings),[7,13] those applicable in ATRPP for the preparation of uniform polymer microspheres are relatively lower, which might be ascribed to their different particle formation mechanism, as discussed in the later section.

(3). Effects of Initiator and Catalyst Concentrations. An important standard for the choice of appropriate initiator and catalyst concentrations is that they can offer a reasonable polymerization rate and at the same time afford narrow-disperse polymer microspheres. The effects of initiator and catalyst concentrations on the morphologies and yields of the polymer microspheres were thus studied with the other polymerization parameters being remained constant (Table 1, entries 14−21). The polymerization rates were found to increase with increasing both the initiator and catalyst concentrations, as indicated by their increased polymer yields, which is understandable because the increase in initiator and catalyst concentrations should lead to the acceleration in the polymerization rates in such a highly diluted polymerization system.[55] In addition, narrow or monodisperse polymer microspheres with smooth surfaces were readily obtained in all the studied initiator and catalyst concentrations (Figure 1c and Figures S4a-d and S5a-d in the Supporting Information), and their sizes increased with increasing the initiator and catalyst concentrations. According to Horák and co-workers,[57] increasing the initiator concentration in the precipitation polymerization system can result in an increase in the instantaneous concentration of growing oligomeric radicals, which in turn increases the rate of oligomer association and the coagulation rate of the unstable primary nuclei to form larger permanent particle nuclei, thus leading to larger final particles. Similar situation should also be expected for the increase in catalyst concentration in ATRPP.

(4). Effect of Molar Ratio of EGDMA to 4-VP. It has been demonstrated that the presence of a divinyl cross-linking monomer is necessary for the preparation of polymer microspheres by precipitation polymerization and its molar ratio to monovinyl monomer has a significant influence on the morphologies of the resulting polymer particles.[7,8,13−16] To check whether it is also applicable in ATRPP, a series of experiments with different molar ratios of EGDMA to 4-VP were also carried out with the molar ratio of vinyl groups in the monomers (including both EGDMA and 4-VP) to initiator to catalyst and other polymerization parameters being held constant (Table 1, entries 22−25). Figure S6 (in the Supporting Information) shows the SEM images of the resulting polymer particles. It can be seen clearly that polydisperse polymer particles were obtained with a molar ratio of EGDMA to 4-VP being 1, while narrow or monodisperse polymer microspheres were formed when the molar ratio of EGDMA to 4-VP ranged from 2 to 4. Similar phenomena were also observed by others in the traditional precipitation polymerization systems and the lower molar ratio of EGDMA to 4-VP was considered to delay the formation of particle nuclei and extend the particle nucleation process, thus resulting in polymer particles with broad size distributions.[13] The D_n values of the resulting polymer microspheres were found to decrease from 2.96 to 2.82 μm with increasing the molar ratio of EGDMA to 4-VP from 2 to 4, which could be ascribed to the formation of a larger number of polymer nuclei in the initial stage of polymerization with increasing the cross-linker loadings, thus decreasing the sizes of the resulting polymer particles.[13] In addition, the yields of the polymer microspheres increased with an increase in EGDMA concentration in the ATRPP system, just as expected. Note that the ATRPP of pure EGDMA led to the sticking of polymer particles to the wall of the reaction flask, thus resulting in polydisperse polymer microspheres (figure not shown). A similar phenomenon was also observed previously in other precipitation polymerization systems.[8,23]

(5). Effect of Reaction Scale. It is extremely important for ATRPP to be scalable in order to prepare enough polymer microspheres in one batch for practical applications. Therefore, a series of experiments with different scales were performed to study the effect of reaction scale on the morphologies and yields of the polymer microspheres (entries 26−28 in Table 1). Note that round-bottom flasks with different volumes (50, 100, and 250 mL) and oval-shaped stir bars with different length (1.5, 2.8, and 2.8 cm) were utilized for different reaction scales (corresponding to entries 26, 27, and 28, respectively) in order to have enough room to hold different volumes of polymerization mixtures and homogeneously disperse the polymer particles in the reaction media. As can be seen clearly from Figure 1d and Figure S7, monodisperse polymer microspheres could be obtained in all the studied reaction scales and their polydispersity indices U and coefficients of variation CV were almost the same within the experimental error (Table 1). However, both the sizes and yields of the polymer microspheres decreased with an increase in the reaction scales. This might be attributed to the different sizes of the reaction flasks and the stir bars used, which might influence the agitation situation for different reactions, thus leading to their different particle sizes and yields. Changing the magnetic stirring to the homogeneous rotation of the polymerization mixtures (as used by Stöver and co-workers[7−12,17]) might be able to solve the above problem.

General Applicability of ATRPP. Narrow or monodisperse cross-linked copolymer microspheres with designed surface functionalities are of considerable interest because they are highly useful for further surface modification and are promising in many materials science applications.[5] It has been demonstrated, however, that precipitation polymerization approach is quite sensitive to the functional comonomers being added into the system. The introduction of certain amounts of hydrophilic functional comonomers into the precipitation polymerization system might result in the mismatch of the solubility parameters between the reaction solvent and the formed polymers, which makes it difficult to obtain monodisperse hydrophilic polymer microspheres with good spherical shape.[18,24] Many efforts have been devoted in this respect and some uniform highly cross-linked copolymer microspheres with incorporated hydrophilic comonomers such as methacrylic acid,[3,18,56] HEMA,[8] and AAm[16] have been prepared via traditional free radical precipitation polymerization through optimizing the polymerization parameters.

To demonstrate its general applicability, ATRPP was performed to prepare highly cross-linked copolymer microspheres with incorporated hydrophilic functional monomers (i.e., HEMA and AAm) (entries 35 and 36 in Table 1). Both narrow-disperse poly(HEMA-*co*-EGDMA) (HEMA/EGDMA =1/2, molar ratio) and monodisperse poly(AAm-*co*-EGDMA) (AAm/EGDMA = 1/4, molar ratio) microspheres were readily obtained following a similar procedure as that used for the preparation of poly(4-VP-*co*-EGDMA) microspheres (Figures 2a,b). The D_n values of poly(HEMA-*co*-EGDMA) and poly(AAm-*co*-EGDMA) microspheres were 1.25 and 2.60 μm, respectively, their U values were

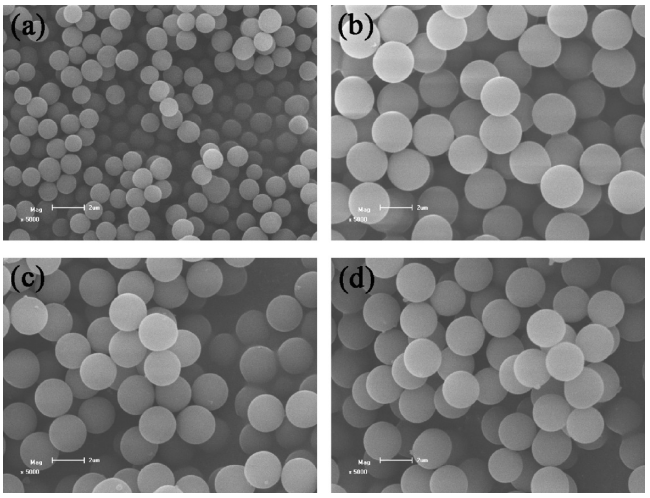

Figure 2. SEM images of poly(HEMA-*co*-EGDMA) (HEMA/EGDMA = 1/2, molar ratio) (a), poly(AAm-*co*-EGDMA) (AAm/EGDMA = 1/4, molar ratio) (b), PNIPAAm brushes-grafted poly(4-VP-*co*-EGDMA) (c), and PHEMA brushes-grafted poly(4-VP-*co*-EGDMA) (d) microspheres, respectively. The scale bar corresponds to 2 μm in parts a−d.

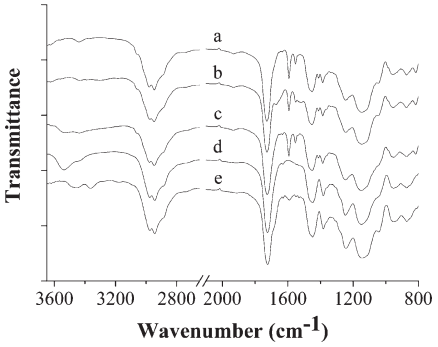

Figure 3. FT-IR spectra of poly(4-VP-*co*-EGDMA) (a), PNIPAAm brushes-grafted poly(4-VP-*co*-EGDMA) (b), PHEMA brushes-grafted poly(4-VP-*co*-EGDMA) (c), poly(HEMA-*co*-EGDMA) (d), and poly(AAm-*co*-EGDMA) (e) microspheres, respectively.

1.024 and 1.005, respectively, and their CV values were 8.9 and 4.1%, respectively. Note that the polymerization parameters for the preparation of poly(HEMA-*co*-EGDMA) and poly(AAm-*co*-EGDMA) microspheres were not optimized in the present study, which further indicates that ATRPP is indeed a highly facile and efficient approach to preparing various surface-functionalized copolymer microspheres with uniform sizes.

FT-IR was first utilized to confirm the successful incorporation of functional comonomers into the obtained polymer microspheres. Figure 3 shows that in addition to the peaks corresponding to the incorporated poly(EGDMA) (i.e., 1725 (C═O stretching), 1247 and 1148 cm^{-1} (C−O−C stretching)), some characteristic peaks of poly(4-VP) such as the C═N stretching (1592 and 1555 cm^{-1}) and C═C stretching (1455 cm^{-1}), those corresponding to poly(AAm) such as the symmetrical and asymmetric N−H stretching bands (around 3360 and 3180 cm^{-1}, respectively) and N−H bending bands (around 1592 cm^{-1}), and those of poly(HEMA) such as the O−H stretching band (around 3540 cm^{-1}) were also clearly observed in the spectra of poly(4-VP-*co*-EGDMA), poly(AAm-*co*-EGDMA), and poly(HEMA-*co*-EGDMA) microspheres,

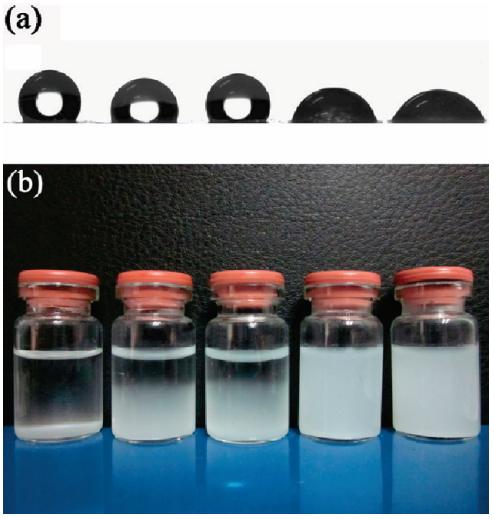

Figure 4. (a) Profiles of a water drop on the films prepared with a series of polymer microspheres; (b) Photograph for the dispersion of polymer microspheres in pure water (1 mg/mL) at 20 °C (after settling down for 2 h). The samples located from left to right in the above two figures are poly(4-VP-*co*-EGDMA), poly(AAm-*co*-EGDMA), poly(HEMA-*co*-EGDMA), PHEMA brushes-grafted poly(4-VP-*co*-EGDMA), and PNIPAAm brushes-grafted poly(4-VP-*co*-EGDMA) microspheres, respectively.

respectively, demonstrating the presence of the bonded functional monomers in the obtained polymer microspheres.

The incorporation of hydrophilic functional comonomers into polymer particles has proven to be an efficient approach to improving their surface hydrophilicity.[58] Moreover, it has been demonstrated that the surface hydrophilicity of the polymer microspheres can be accurately evaluated by performing water contact angle experiments.[34] Therefore, the static water contact angles of the films prepared with polymer microspheres bearing incorporated 4-VP, HEMA, and AAm were determined in order to get more insight into their surface properties. Figure 4a shows the profiles of a water drop on the films of the studied polymer microspheres, from which the static water contact angles of the films prepared with poly(4-VP-*co*-EGDMA), poly(HEMA-*co*-EGDMA), and poly(AAm-*co*-EGDMA) microspheres were determined to be 124, 110, and 101°, respectively. The relatively lower static water contact angles for the films made from poly(HEMA-*co*-EGDMA) and poly(AAm-*co*-EGDMA) microspheres in comparison with that prepared with poly(4-VP-*co*-EGDMA) microspheres further confirmed the successful incorporation of hydrophilic monomers into these polymer microspheres.

The dispersion stability of poly(4-VP-*co*-EGDMA), poly(HEMA-*co*-EGDMA), and poly(AAm-*co*-EGDMA) microspheres in water was also studied to test their surface wettability (Figure 4b, Figure S8). Much faster sedimentation was observed for poly(4-VP-*co*-EGDMA) microspheres in comparison with poly(HEMA-*co*-EGDMA) and poly(AAm-*co*-EGDMA) microspheres, revealing the improved surface hydrophilicity for poly(HEMA-*co*-EGDMA) and poly(AAm-*co*-EGDMA) microspheres and thus the successful incorporation of hydrophilic functional comonomers into these polymer microspheres.

"Livingness" of the Polymer Microspheres Prepared by ATRPP. It is well-known that one of the main advantages that CRPs can offer is their versatility in preparing well-defined polymers with end-capped "living" groups, which makes their further chain extension possible.[35−38] Therefore, the introduction of

ATRP mechanism into precipitation polymerization is expected to provide "living" polymer microspheres with reactive ATRP initiating groups on their surfaces. To confirm this hypothesis, the above-obtained polymer microspheres were utilized as the immobilized ATRP initiator for the surface-initiated ATRP of hydrophilic functional monomers (i.e., NIPAAm and HEMA).

The surface-initiated ATRP of NIPAAm was first carried out in isopropanol at 25 °C for 24 h under the magnetic stirring with sample entry 28 in Table 1 (Figure 1d: D_n = 2.38, U = 1.008, CV = 5.3%) as the immobilized ATRP initiator and $CuCl/CuCl_2/Me_6TREN$ as the catalyst. No free initiator was added into the polymerization system, which means that the polymerization should be surface-confined. $CuCl_2$ ($CuCl_2/CuCl$ = 0.10) was added into the polymerization solution to improve the controllability of the polymerization system.[55,59] A weight increase of 10% was observed for the polymer particles after their surface modification, indicating that PNIPAAm brushes were grafted onto the polymer particles. The SEM investigation showed that the modified polymer particles were still separate microspheres, with their D_n and U values being 2.41 μm and 1.005, respectively (Figure 2c). An increase of about 30 nm in D_n value was observed for the grafted polymer microspheres in comparison with the ungrafted ones, again revealing the successful grafting of PNIPAAm brushes onto the polymer microspheres via the surface-initiated ATRP.

Surface-initiated ATRP of HEMA was then performed in methanol/water (1/1 v/v) at ambient temperature for 24 h under the magnetic stirring with the same sample entry 28 in Table 1 as the immobilized ATRP initiator and $CuCl/CuBr_2$/2,2′-bipyridine as the catalyst. A weight increase of 12% was observed for the polymer particles after their surface modification. The grafted polymer particles also proved to be separate microspheres, with their D_n and U being 2.41 μm and 1.004, respectively (Figure 2d). An increase of about 30 nm in D_n value was observed for the grafted polymer particles in comparison with the ungrafted ones. The above results demonstrate the successful grafting of PHEMA brushes onto the polymer microspheres. It is important to stress here that the increased weights of the grafted polymer microspheres should be mainly stemmed from the surface-grafted polymer brushes because the use of poor solvents for the "living" polymer microspheres in the grafting polymerization processes and their rather high cross-linking densities would prevent them from swelling in the reaction media and only allow the occurrence of surface polymerization, just as reported by Tirelli and co-workers.[60]

To confirm the occurrence of only surface polymerization during the above surface-initiated ATRP of hydrophilic monomers, the polymer microspheres grafted with PHEMA brushes were allowed to react with a carboxyl group-containing fluorescent dye Rhodamine B in THF under the catalysis of DCC/DMAP. The control labeling experiment was also performed for the ungrafted polymer microspheres under the same reaction condition. After being thoroughly washed with solvents, the obtained polymer microspheres were studied with confocal microscopy, which can provide image depth and enable the fabrication of cross-sectional slices of the images.[31] Figure S8a (in the Supporting Information) represents a cross-sectional slice of the Rhodamine B-labeled polymer microspheres grafted with PHEMA brushes, which clearly shows the fluorescence only in the outer shell and no fluorescence in the core of the particle. This, together with the absence of any fluorescence for the ungrafted polymer microspheres after their control labeling treatment (Figure S8b), definitely confirmed the grafting of polymer brushes only on the surfaces of the grafted polymer microspheres and their core−shell structures.

FT-IR was employed to further verify the successful grafting of PNIPAAm and PHEMA brushes onto the polymer microspheres (Figure 3). For the ungrafted poly(4-VP-*co*-EGDMA) microspheres, the absorption peaks characteristic of the bonded EGDMA appeared at 1728 (C═O stretching) and 1245/1148 cm^{-1} (C−O−C stretching), while those corresponding to the C═N stretching (1592 and 1555 cm^{-1}) and C═C stretching (1455 cm^{-1}) for the bonded 4-VP were also clearly discernible. In addition to the above absorption peaks, some new ones characteristic of PNIPAAm (i.e., the amide I band (1668 cm^{-1}, C═O stretching) and amide II band (1528 cm^{-1}, N−H stretching)) and PHEMA (3540 cm^{-1}, O−H stretching) were also observed in the FT-IR spectra of the polymer microspheres obtained via the surface-initiated ATRP of NIPPAm and HEMA, respectively, again demonstrating the successful grafting of PNIPAAm and PHEMA brushes.

Surface-grafting of hydrophilic polymer brushes has proven to be a highly effective approach to improving the surface hydrophilicity and water dispersion stability of the polymer microspheres.[34] Therefore, it is expected that the polymer particles grafted with PNIPAAm and PHEMA brushes should show much reduced static water contact angles and enhanced dispersion stability in water. The results shown in Figure 4, parts a and b, indeed support this hypothesis. The static water contact angles of the films prepared with polymer microspheres bearing PNIPAAm and PHEMA brushes were determined to be 67 and 73°, respectively, which were significantly lower than that (124°) of the film prepared with the ungrafted poly(4-VP-*co*-EGDMA) microspheres. In addition, there was much faster sedimentation for the ungrafted polymer microspheres in water in comparison with the grafted ones (Figure S9, Supporting Information). These results provide strong evidence for the presence of PNIPAAm and PHEMA brushes on the surfaces of the grafted microspheres. Furthermore, the results also revealed that in comparison with the polymer microspheres with incorporated hydrophilic functional monomers (i.e., poly(HEMA-*co*-EGDMA) and poly(AAm-*co*-EGDMA) microspheres), the polymer microspheres with grafted hydrophilic polymer brushes exhibited much higher surface hydrophilicity and significantly improved water dispersion stability.

Proposed Particle Formation Mechanism in ATRPP. According to Stöver and co-workers,[9] the particle formation mechanism in the traditional precipitation polymerization includes particle nucleation and growth stages, where the nucleation process occurrs by the aggregation of oligomers to form particle nuclei at the beginning of the polymerization and the subsequent particle growth process mainly involves the capture of oligomeric radicals from the reaction medium by their reacting with the residual vinyl groups on the surfaces of the existing particles. Being similar to traditional precipitation polymerization, ATRPP should also involve the typical particle nucleation and growth stages. It starts from a homogeneously mixed solution of dinvinyl cross-linker, monvinyl functional monomer, initiator, catalyst (copper halide and a ligand), and a large amount of solvent. When ATRPP is activated under appropriate reaction conditions, all chains are quickly initiated and grow simultaneously, leading to soluble branched oligomers at the beginning of the polymerization.[61] As these branched oligomer chains grow beyond their solubility limit in the reaction medium, they will

Scheme 1. Proposed Particle Formation Mechanism in ATRPP, Which Involves the Particle Nucleation (a−c) and Particle Growth (d) Processes

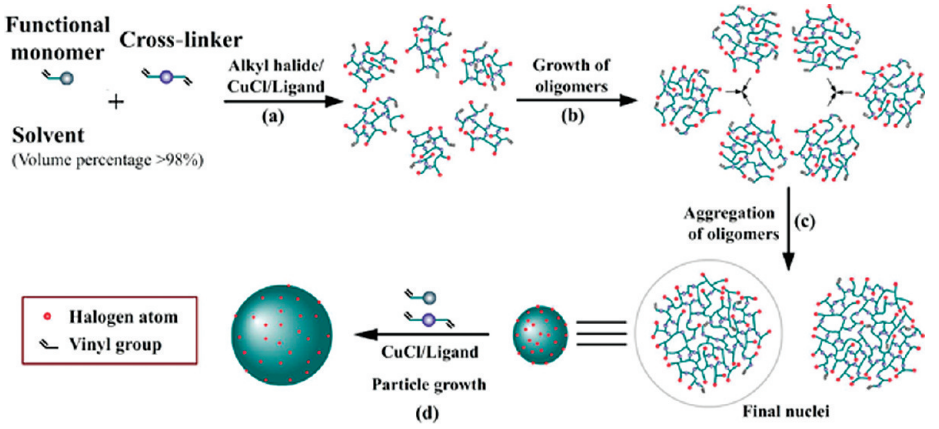

precipitate out of the continuous medium and their subsequent aggregation eventually leads to the formation of particle nuclei (with surface-immobilized ATRP initiating groups), which then increase their sizes following the polymerization process. According to the ATRP mechanism, all the ATRP initiators in the ATRPP system should be rapidly transformed into macroinitiators soon after the polymerization starts, which means that the amount of newly formed polymer chains in the reaction medium during the particle growth stage should be negligible. This is in sharp contrast with the traditional precipitation polymeriztaion system, where new oligmers are continuously generated in the continuous phase due to the presence of traditional initiating species (e.g., AIBN) in the reaction medium throughout the polymerization process. Therefore, the particle growth mechanism in ATRPP should be considerably different from that of the traditional precipitation polymerization. While the particle growth in the traditional precipitation polymerization system occurrs mainly by an entropic precipitation mechanism where soluble oligomer radical species are continuously captured from the solution by their reacting with the pendant vinyl groups on the surfaces of the existing particles,[9,11,12,17] the polymer particles in the ATRPP system grow only by directly capturing monomers (including both divinyl cross-linkers and monovinyl functional monomers) from the reaction solution through the surface-initiated controlled polymerization process. Therefore, if we use the grafting concept described in the Introduction (the second paragraph) and define the particle growth mechainsm in the traditional precipitation polymerization as a "grafting to" mechanism, a "grafting from" growth mechanism should work in ATRPP. Scheme 1 schematically outlines the above proposed particle formation mechanism in ATRPP. It is apparent that the controlled characteristics of ATRPP should lead to uniform particle growth, good control over particle sizes, and uniformly cross-linked polymer networks.[44,53,61] More importantly, all the resulting polymer microspheres by ATRPP should contain active ATRP initiating groups on their surfaces, which is of great importance for their further surface functionalization.

To get more insight into ATRPP, a series of time-dependent ATRPP experiments were carried out to trace the whole polymerization process (Table 1, entries 29−34). The polymerization solutions were found to turn from a transparent clear solution to a slightly turbid state at a polymerization time of about 1.5 h,

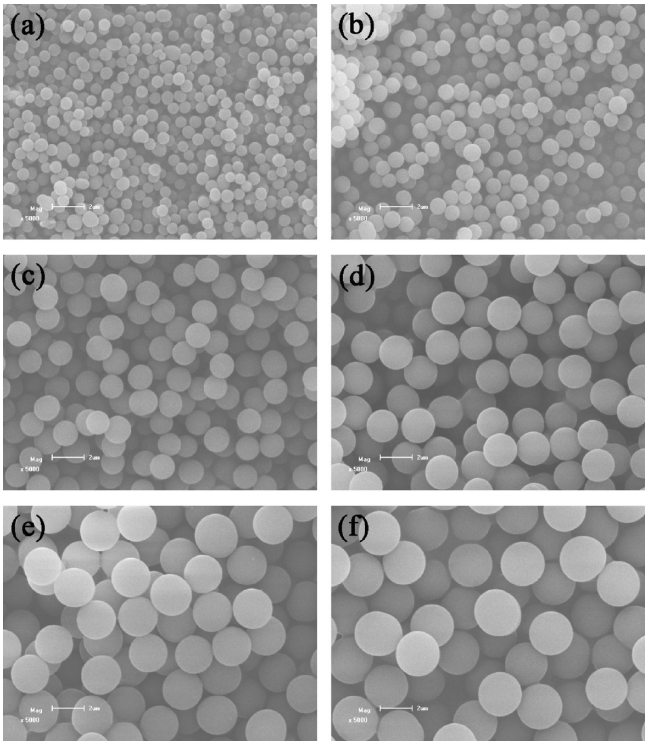

Figure 5. SEM images of poly(4-VP-*co*-EGDMA) microspheres prepared via ATRPP at a polymerization time of 2 (a), 3 (b), 6 (c), 12 (d), 18 (e), and 24 h (f), respectively (the reaction conditions are listed in entries 29−34 in Table 1). The scale bar corresponds to 2 μm in parts a−f.

indicating the occurrence of the particle nucleation process. Figure 5 shows the SEM images of poly(4-VP-*co*-EGDMA) microspheres obtained at different polymerization times. It is interesting to note that polymer microspheres with rather uniform sizes ($U \leq 1.022$) were obtained even at the beginning of the polymerization (although some particles with irregular shapes were observed at a polymerization time of 2 h), which is considerably different from many traditional precipitation polymerization systems, where highly polydisperse uneven polymer particles were produced at the early stage of the polymerization.[20,21,23] In addition,

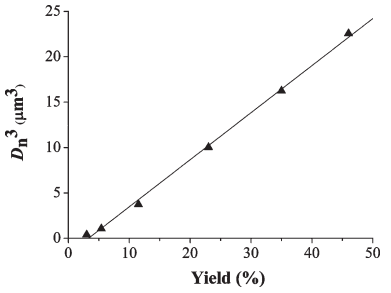

Figure 6. Plot of the cubes of the number-average diameters of poly(4-VP-*co*-EGDMA) microspheres prepared via ATRPP at different polymerization times versus their yields.

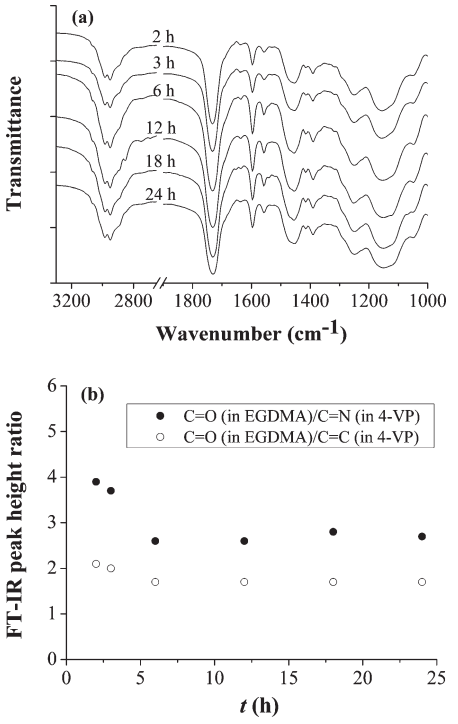

Figure 7. (a) FT-IR spectra of poly(4-VP-*co*-EGDMA) microspheres prepared via ATRPP at a polymerization time of 2, 3, 6, 12, 18, and 24 h, respectively; (b) The FT-IR peak height ratio of C═O stretching band from the bonded EGDMA to C═N or C═C stretching band from the bonded 4-VP (which refers to the bonded amount of EGDMA relative to that of 4-VP) in poly(4-VP-*co*-EGDMA) microspheres prepared via ATRPP at different polymerization times.

the yields, sizes, and uniformity of the polymer microspheres increased with increasing the polymerization time. For example, the yields of the polymer microspheres increased from 3 to 46% with increasing the polymerization time from 2 to 24 h; the D_n and U values of the polymer microspheres obtained at a polymerization time of 2 h were 0.73 μm and 1.022, respectively, while those of the polymer microspheres obtained at a polymerization time of 24 h were 2.83 μm and 1.004, respectively. More importantly, a very good linear relationship between the yields and the cubes of D_n of the polymer microspheres was obtained for the studied system (Figure 6), demonstrating that the number of polymer particles remained constant during the ATRPP process and neither coagulation nor secondary nucleation occurred after the nucleation process.[13]

Figure 7a presents the FT-IR spectra of poly(4-VP-*co*-EGDMA) microspheres obtained at different polymerization times, from which the incorporated levels of EGDMA and 4-VP in the polymer microspheres can be readily derived by comparing the peak height for the C═O band from the bonded EGDMA (1730 cm^{-1}) with that for the C═N stretching band (around 1595 cm^{-1}) or C═C stretching band (1456 cm^{-1}) from the bonded 4-VP (Figure 7b).[34] It can be seen clearly that the amount of the bonded EGDMA relative to the bonded 4-VP in the polymer microspheres decreased with increasing the polymerization time at the early stage of the ATRPP process, while it leveled off at a polymerization time ≥6 h. The above results suggested that a relatively higher level of EGDMA might be incorporated into the polymer particles during the nucleation process (in comparsion with that incorporated during the particle growth process), while homogeneous grafting of a constant amount of EGDMA and 4-VP molecules onto the polymer microspheres took place during most of the particle growth period, which should lead to the formation of a unformly cross-linked network around the polymer nuclei in the polymer microspheres prepared via ATRPP.[39,49,53,54] Note that the uniform grafting of EGDMA and 4-VP molcules onto the polymer microspheres during the particle growth process in ATRPP might provide polymer microspheres with a more compact surface layer in comparison with those prepared via traditional precipitation polymerization (which have a lightly cross-linked transient solvent-sowllen gel layers on the particle surfaces due to their capturing of soluble oligomers[9]). Therefore, the polymer particles generated in ATRPP should be less stabilized in the reaction media than those generated in traditional precipitation polymerization, which might account for the relatively lower monomer loadings in ATRPP for the preparation of narrow or monodisperse polymer microspheres.

CONCLUSION

We have developed a facile, general, and highly efficient approach to obtaining narrow or monodisperse, highly cross-linked, surface-functionalized, and "living" polymer microspheres with uniformly cross-linked structures by ATRPP. Polymer microspheres with their sizes ranging from 0.73 to 3.25 μm and their polydispersity indices being typically lower than 1.01 were readily prepared and their sizes could be easily tailored by tuning the polymerization parameters. The general applicability of ATRPP was demonstrated by preparing a series of uniform copolymer microspheres with different incorporated functional monomers. In addition, the "livingness" of the resulting polymer microspheres was also confirmed by their easy surface modification via the surface-initiated ATRP of hydrophilic functional monomers, leading to polymer brushes-grafted polymer microspheres with significantly enhanced surface hydrophilicity and water dispersion stability. Furthermore, a "grafting from" particle growth mechanism was proposed for the ATRPP system, which is considerably different from the "grafting to" particle growth mechanism in the traditional precipitation polymerization. In view of the great versatility of ATRP (such as its compatibility to a wide range of functional monomers and its very mild reaction conditions) in the controlled surface modification of various substrate materials, we believe that such advanced functional "living" polymer microspheres presented here hold enormous potential for a diverse range of applications in the field of materials science. The research on the preparation of monodisperse

polymer microspheres with surface-grafted more complexed polymer structures (e.g., block polymer brushes) from these "living" polymer microspheres is currently ongoing in our laboratories.

■ ASSOCIATED CONTENT

Supporting Information. SEM images of poly(4-VP-*co*-EGDMA) microspheres prepared via ATRPP under different polymerization conditions, confocal microscopy images of Rhodamine B-labeled polymer microspheres grafted with PHEMA brushes and the ungrafted polymer microspheres after their control labeling treatment, and the detailed photographs for the water dispersion stability of polymer microspheres. This material is available free of charge via the Internet at http://pubs.acs.org.

■ AUTHOR INFORMATION

Corresponding Author

*Telephone/Fax: +86-2223507193. E-mail: zhanghuiqi@nankai.edu.cn.

■ ACKNOWLEDGMENT

The authors express thanks for the financial support from National Natural Science Foundation of China (20744003, 20774044), Natural Science Foundation of Tianjin (06YFJMJC15100, 11JCYBJC01500), a supporting program for New Century Excellent Talents (Ministry of Education) (NCET-07-0462), and a start-up fund from Nankai University. Professor Yakai Feng (School of Chemical Engineering and Technology, Tianjin University, People's Republic of China) is thanked for his kind help in measuring the static water contact angles of the samples.

■ REFERENCES

(1) Horák, D. *Acta Polym.* **1996**, *47*, 20–28.
(2) Xia, Y.; Gates, B.; Yin, Y.; Lu, Y. *Adv. Mater.* **2000**, *12*, 693–713.
(3) Wang, J.; Cormack, P. A. G.; Sherrington, D. C.; Khoshdel, E. *Angew. Chem., Int. Ed.* **2003**, *42*, 5336–5338.
(4) Ye, L.; Mosbach, K. *Chem. Mater.* **2008**, *20*, 859–868.
(5) Barner, L. *Adv. Mater.* **2009**, *21*, 2547–2553.
(6) Naka, Y.; Kaetsu, I.; Yamamoto, Y.; Hayashi, K. *J. Polym. Sci., Part A: Polym. Chem.* **1991**, *29*, 1197–1202.
(7) Li, K.; Stöver, H. D. H. *J. Polym. Sci., Part A: Polym. Chem.* **1993**, *31*, 3257–3263.
(8) Li, W. H.; Stöver, H. D. H. *J. Polym. Sci., Part A: Polym. Chem.* **1999**, *37*, 2899–2907.
(9) Downey, J.; Frank, R. S.; Li, W. H.; Stöver, H. D. H. *Macromolecules* **1999**, *32*, 2838–2844.
(10) Li, W. H.; Stöver, H. D. H. *Macromolecules* **2000**, *33*, 4354–4360.
(11) Downey, J.; McIsaac, G.; Frank, R. S.; Stöver, H. D. H. *Macromolecules* **2001**, *34*, 4534–4541.
(12) Frank, R. S.; Downey, J.; Yu, K.; Stöver, H. D. H. *Macromolecules* **2002**, *35*, 2728–2735.
(13) Bai, F.; Yang, X.; Huang, W. *Macromolecules* **2004**, *37*, 9746–9752.
(14) Yang, S.; Shim, S. E.; Lee, H.; Kim, G. P.; Choe, S. *Macromol. Res.* **2004**, *12*, 519–527.
(15) Shim, S. E.; Yang, S.; Choe, S. *J. Polym. Sci., Part A: Polym. Chem.* **2004**, *42*, 3967–3974.
(16) Jin, J. M.; Yang, S.; Shim, S. E.; Choe, S. *J. Polym. Sci., Part A: Polym. Chem.* **2005**, *43*, 5343–5346.
(17) Takekoh, R.; Li, W. H.; Burke, N. A. D.; Stöver, H. D. H. *J. Am. Chem. Soc.* **2006**, *128*, 240–244.
(18) Bai, F.; Yang, X.; Li, R.; Huang, B.; Huang, W. *Polymer* **2006**, *47*, 5775–5784.
(19) Joso, R.; Pan, E. H.; Stenzel, M. H.; Davis, T. P.; Barner-Kowollik, C.; Barner, L. *J. Polym. Sci., Part A: Polym. Chem.* **2007**, *45*, 3482–3487.
(20) Limé, F.; Irgum, K. *Macromolecules* **2007**, *40*, 1962–1968.
(21) Yan, Q.; Bai, Y.; Meng, Z.; Yang, W. *J. Phys. Chem. B* **2008**, *112*, 6914–6922.
(22) Yan, Q.; Zhao, T.; Bai, Y.; Zhang, F.; Yang, W. *J. Phys. Chem. B* **2009**, *113*, 3008–3014.
(23) Limé, F.; Irgum, K. *Macromolecules* **2009**, *42*, 4436–4442.
(24) Medina-Castillo, A. L.; Fernandez-Sanchez, J. F.; Segura-Carretero, A.; Fernandez-Gutierrez, A. *Macromolecules* **2010**, *43*, 5804–5813.
(25) Zheng, G.; Stöver, H. D. H. *Macromolecules* **2002**, *35*, 6828–6834.
(26) Zheng, G.; Stöver, H. D. H. *Macromolecules* **2002**, *35*, 7612–7619.
(27) Zheng, G.; Stöver, H. D. H. *Macromolecules* **2003**, *36*, 1808–1814.
(28) Zheng, G.; Stöver, H. D. H. *Macromolecules* **2003**, *36*, 7439–7445.
(29) Barner, L.; Li, C.; Hao, X.; Stenzel, M. H.; Barner-Kowollik, C.; Davis, T. P. *J. Polym. Sci., Part A: Polym. Chem.* **2004**, *42*, 5067–5076.
(30) Joso, R.; Stenzel, M. H.; Davis, T. P.; Barner-Kowollik, C.; Barner, L. *Aust. J. Chem.* **2005**, *58*, 468–471.
(31) Goldmann, A. S.; Walther, A.; Nebhani, L.; Joso, R.; Ernst, D.; Loos, K.; Barner-Kowollik, C.; Barner, L.; Müller, A. H. E. *Macromolecules* **2009**, *42*, 3707–3714.
(32) Yang, K.; Berg, M. M.; Zhao, C.; Ye, L. *Macromolecules* **2009**, *42*, 8739–8746.
(33) Li, J.; Zu, B.; Zhang, Y.; Guo, X.; Zhang, H. *J. Polym. Sci., Part A: Polym. Chem.* **2010**, *48*, 3217–3228.
(34) Pan, G.; Zhang, Y.; Guo, X.; Li, C.; Zhang, H. *Biosens. Bioelectron.* **2010**, *26*, 976–982.
(35) Hawker, C. J.; Bosman, A. W.; Harth, E. *Chem. Rev.* **2001**, *101*, 3661–3688.
(36) Matyjaszewski, K.; Xia, J. *Chem. Rev.* **2001**, *101*, 2921–2990.
(37) Kamigaito, M.; Ando, T.; Sawamoto, M. *Chem. Rev.* **2001**, *101*, 3689–3746.
(38) Moad, G.; Rizzardo, E.; Thang, S. H. *Polymer* **2008**, *49*, 1079–1131.
(39) Oh, J. K.; Tang, C.; Gao, H.; Tsarevsky, N. V.; Matyjaszewski, K. *J. Am. Chem. Soc.* **2006**, *128*, 5578–5584.
(40) Song, J. S.; Winnik, M. A. *Macromolecules* **2006**, *39*, 8318–8325.
(41) Zheng, G.; Pan, C. *Macromolecules* **2006**, *39*, 95–102.
(42) Wan, W.; Pan, C. *Macromolecules* **2007**, *40*, 8897–8905.
(43) An, Z.; Shi, Q.; Tang, W.; Tsung, C. K.; Hawker, C. J.; Stucky, G. D. *J. Am. Chem. Soc.* **2007**, *129*, 14493–14499.
(44) Min, K.; Matyjaszewski, K. *Macromolecules* **2007**, *40*, 7217–7222.
(45) Thurecht, K. J.; Gregory, A. M.; Wang, W.; Howdle, S. M. *Macromolecules* **2007**, *40*, 2965–2967.
(46) Grignard, B.; Jérôme, C.; Calberg, C.; Jérôme, R.; Wang, W.; Howdle, S. M.; Detrembleur, C. *Macromolecules* **2008**, *41*, 8575–8583.
(47) Min, K.; Gao, H.; Yoon, J. A.; Wu, W.; Kowalewski, T.; Matyjaszewski, K. *Macromolecules* **2009**, *42*, 1597–1603.
(48) Shen, W.; Chang, Y.; Liu, G.; Wang, H.; Cao, A.; An, Z. *Macromolecules* **2011**, *44*, 2524–2530.
(49) Pan, G.; Zu, B.; Guo, X.; Zhang, Y.; Li, C.; Zhang, H. *Polymer* **2009**, *50*, 2819–2825.
(50) Otsu, T. *J. Polym. Sci., Part A: Polym. Chem.* **2000**, *38*, 2121–2136.
(51) Ciampolini, M.; Nardi, N. *Inorg. Chem.* **1966**, *5*, 41–44.
(52) Pyun, J.; Kowalewski, T.; Matyjaszewski, K. *Macromol. Rapid Commun.* **2003**, *24*, 1043–1059.
(53) Huang, W.; Baker, G. L.; Bruening, M. L. *Angew. Chem., Int. Ed.* **2001**, *40*, 1510–1512.

(54) Zu, B.; Pan, G.; Guo, X.; Zhang, Y.; Zhang, H. *J. Polym. Sci., Part A: Polym. Chem.* **2009**, *47*, 3257–3270.
(55) Zhang, H.; Klumperman, B.; Ming, W.; Fischer, H.; Van der Linde, R. *Macromolecules* **2001**, *34*, 6169–6173.
(56) Ye, L.; Weiss, R.; Mosbach, K. *Macromolecules* **2000**, *33*, 8239–8245.
(57) Macková, H.; Horák, D. *J. Polym. Sci., Part A: Polym. Chem.* **2006**, *44*, 968–982.
(58) Dirion, B.; Cobb, Z.; Schillinger, E.; Andersson, L. I.; Sellergren, B. *J. Am. Chem. Soc.* **2003**, *125*, 15101–15109.
(59) Huang, W.; Kim, J. B.; Bruening, M. L.; Baker, G. L. *Macromolecules* **2002**, *35*, 1175–1179.
(60) Bontempo, D.; Tirelli, N.; Feldman, K.; Masci, G.; Crescenzi, V.; Hubbell, J. A. *Adv. Mater.* **2002**, *14*, 1239–1241.
(61) Gao, H.; Matyjaszewski, K. *Prog. Polym. Sci.* **2009**, *34*, 317–350.